Abnormal Salience Network in Normal Aging and in Amnestic Mild Cognitive Impairment and Alzheimer's Disease

Xiaoxi He,[1†] Wen Qin,[1†] Yong Liu,[2,3†] Xinqing Zhang,[4] Yunyun Duan,[5] Jinyu Song,[1] Kuncheng Li,[5] Tianzi Jiang,[2,3] and Chunshui Yu[1]*

[1]Department of Radiology and Tianjin Key Laboratory of Functional Imaging, Tianjin Medical University General Hospital, Tianjin 300052, China
[2]Brainnetome Center, Institute of Automation, Chinese Academy of Sciences, Beijing 100190, China
[3]National Laboratory of Pattern Recognition, Institute of Automation, Chinese Academy of Sciences, Beijing 100190, China
[4]Department of Neurology, Xuanwu Hospital, Capital Medical University, Beijing 100053, China
[5]Department of Radiology, Xuanwu Hospital, Capital Medical University, Beijing 100053, China

---

Abstract: The salience network (SN) serves to identify salient stimuli and to switch between the central executive network (CEN) and the default-mode network (DMN), both of which are impaired in Alzheimer's disease (AD)/amnestic mild cognitive impairment (aMCI). We hypothesized that both the structural and functional organization of the SN and functional interactions between the SN and CEN/DMN are altered in normal aging and in AD/aMCI. Gray matter volume (GMV) and resting-state functional connectivity (FC) were analyzed from healthy younger (HYC) to older controls (HOC) and from HOC to aMCI and AD patients. All the SN components showed significant differences in the GMV, intranetwork FC, and internetwork FC between the HYC and HOC. Most of the SN components showed differences in the GMV between the HOC and AD and between the aMCI and AD. Compared with the HOC, AD patients exhibited significant differences in intra- and internetwork FCs of the SN, whereas aMCI patients demonstrated differences in internetwork FC of the SN. Most of the GMVs and internetwork FCs of the SN and part of the intranetwork FC of the SN were correlated with cognitive differences in older subjects. Our findings suggested that structural and functional impairments of the SN may occur as early as in normal aging and that functional disconnection between the SN and

---

INTRODUCTION

The salience network (SN) mainly consists of the dorsal anterior cingulate (dACC) and frontoinsular (FIC) cortices and serves to identify the most relevant stimuli among several internal and external stimuli to guide behavior [Menon and Uddin, 2010; Seeley et al., 2007]. It has been suggested that the right FIC plays a critical role in switching between the central executive network (CEN) and the default-mode network (DMN) [Sridharan et al., 2008], which are known to interact competitively during cognitive information processing [Fox et al., 2005; Greicius et al., 2003]. The FIC serves to identify salient stimuli from the vast and continuous stream of visual, auditory, tactile, and other sensory system inputs. Once a salient stimulus is detected, the FIC initiates the appropriate transient control signals to engage the CEN in mediating attention, working memory and other higher order cognitive processes while disengaging the DMN via the large axons of the von Economo neurons (VENs) [Allman et al., 2005; Menon and Uddin, 2010]. Importantly, this switching mechanism helps to focus attention on external stimuli. As a result, the stimuli take on added significance or saliency [Menon and Uddin, 2010].

The CEN mainly consists of the dorsolateral prefrontal cortex (DLPFC) and posterior parietal cortex (PPC), while the DMN includes the ventromedial prefrontal cortex (VMPFC) and posterior cingulate cortex (PCC) [Damoiseaux et al., 2006]. These two networks can be easily identified by observing their profiles of activation and deactivation during the performance of cognitively demanding tasks. The CEN typically shows increases in activation, whereas the DMN shows decreases in activation [Greicius and Menon, 2004; Greicius et al., 2003; Raichle et al., 2001]. Numerous neuroimaging studies have suggested that the structural and functional organizations of these two networks are impaired in Alzheimer's disease (AD) [Agosta et al., 2011; Binnewijzend et al., 2011; Greicius, 2004; Li et al., 2013] and in normal aging in the absence of disease. Moreover, impairment in these two networks has been associated with a cognitive decline in the aging subjects [Andrews-Hanna et al., 2007]. Because the SN, CEN, and DMN interact closely to control cognitive processes, we hypothesized that the structural and functional organization of the SN and the functional connectivity (FC) between the SN and the other two networks (CEN and DMN) are also altered in AD patients and in normal aging.

Although a pioneering study revealed that AD patients showed increased intranetwork FC in the SN and reduced intranetwork FC in the DMN compared to matched healthy older subjects after atrophy correction, the structural changes in the SN in AD have not been investigated in detail [Zhou et al., 2010]. Patients with AD exhibit progressive atrophy in the whole brain, which enables the prediction of atrophy in the SN in these patients. Moreover, we predict that the structural and functional alterations in the SN are present in normal aging because SN-related functions, such as attention and cognitive control, have been found to be impaired during the process of normal aging. More importantly, alterations in the internetwork FC between the SN and the CEN and DMN in normal aging and AD have not yet been investigated and will be critical in understanding the role of SN deficits in normal aging and in AD. Consequently, in this study, we combined voxel-based morphometry (VBM) and resting-state intranetwork FC analyses to answer the following two questions: (1) the aging question: whether gray matter volume (GMV) and intra- and internetwork FCs of the SN differs between healthy younger (HYC) and older controls (HOC); and (2) the cognitive decline question: whether the GMV and intra- and internetwork FCs of the SN differs among the HOC, patients with amnestic mild cognitive impairment (aMCI), and patients with AD; and whether structural and functional changes in the SN are associated with cognitive differences in older subjects. A schematic summary of the study design is shown in Figure 1.

MATERIALS AND METHODS

Subjects

This study was approved by the Medical Research Ethics Committee of Xuanwu Hospital of Capital Medical University, and written informed consent was obtained from all participants. All patients were consecutively recruited from the memory clinic at Xuanwu Hospital, and the HOC subjects were recruited using advertisements posted in the hospital and in communities near the hospital. All qualified subjects were provided with compensation for their participation. A total of eighty-seven older subjects underwent a standard dementia screening that included the acquisition of a medical history, physical and neurological examinations, laboratory tests, neuropsychological assessments, and brain MRI. Cognitive function was evaluated using the Mini-Mental State Examination
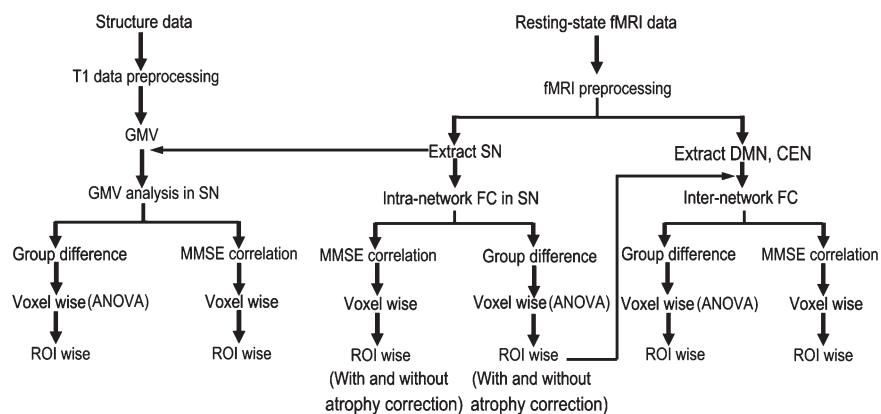
Figure 1.

A schematic summary of the study design. Abbreviations: CEN, central executive network; DMN, default-mode network; FC, functional connectivity; GMV, gray matter volume; MMSE, Mini-Mental State Examination; ROI, region of interest; SN, salience network.

(MMSE) and the degree of dementia was determined using the clinical dementia rating scale (CDR). AD was diagnosed by an experienced neurologist (X.Z.) using the NINCDS-ADRDA (National Institute of Neurological and Communicative Disorders and Stroke and the Alzheimer's Disease and Related Disorders Association) criteria for "probable AD" [McKhann et al., 1984]. aMCI was diagnosed by the same neurologist (X.Z.) according to the criteria for aMCI [Petersen et al., 2001]: (1) memory complaint, preferably confirmed by an informant; (2) objective memory impairment, adjusted for age and education; (3) normal or near-normal performance on general cognitive functioning and no or minimum impairment of daily life activities; (4) a Clinical Dementia Rating (CDR) [Morris, 1993] score of 0.5; and (5) failure to meet the criteria for dementia. Inclusion criteria for these older subjects were as follows: (1) aged 50–90 years; (2) ability to cooperatively finish all tests; (3) no history of stroke; and (4) no more than one lacunar infarction, and no patchy or diffusive leukoaraiosis on conventional MR images. The exclusion criteria included any severe medical condition, other neurological or psychiatric illness, or history of brain injury. In addition, 75 gender-matched HYC subjects (age 18–35 years), who were recruited using advertisements posted at nearby colleges and communities, were included

in the study. Thirteen older subjects were further excluded due to excessive head motion during MR scanning or poor image quality. In total, 75 HYC, 21 HOC, 18 aMCI, and 35 AD patients were included in the analyses. The demographic and neuropsychological data of these subjects are shown in Table I.

Image Acquisition

MR images were acquired on a 3.0 T MR scanner (Magnetom Trio, Siemens, Germany). Resting-state fMRI data were acquired using an echo planar imaging (EPI) sequence with the following scan parameters: repetition time (TR) = 2,000 ms, echo time (TE) = 30 ms, flip angle (FA) = 90°, matrix = 64 × 64, field of view (FOV) = 220 × 220 mm^2, slice thickness = 3 mm, and slice gap = 1 mm. Each brain volume consisted of 32 axial slices and 180 volumes. During the fMRI scans, all subjects were instructed to keep their eyes closed, to stay as motionless as possible, to think of nothing in particular, and to not fall asleep. Sagittal T1-weighted MR images were acquired using a magnetization prepared rapid acquisition gradient echo (MP-RAGE) sequence (TR/TE = 2,000/2.6 ms; FA =

TABLE I. Demographic and neuropsychological characteristics of subjects

Items	HYC ($n = 75$)	HOC ($n = 21$)	aMCI ($n = 18$)	AD ($n = 35$)
Age (mean ± SD; years)	23.8 ± 4.0	65.0 ± 8.2	70.2 ± 7.9	65.8 ± 8.3
Gender (males/females)	38/37	7/14	10/8	17/18
Years of education (mean ± SD)	11.5 ± 5.5	11.0 ± 4.4	9.4 ± 4.8	10.6 ± 4.2
MMSE (mean ± SD)	—	28.5 ± 1.4	21.9 ± 5.0	10.1 ± 6.7
CDR (range)	—	0	0.5	1–3

AD, Alzheimer's disease; aMCI, amnestic mild cognitive impairment; CDR, Clinical Dementia Rating; HOC, healthy older control; HYC, healthy younger control; MMSE, Mini-Mental State Examination; SD, standard deviation.

9°; matrix = 256 × 224; inversion time = 900 ms; slice thickness = 1 mm, no gap; 176 slices).

Preprocessing of Structural MRI

VBM analysis was performed using Statistical Parametric Mapping software (SPM8; http://www.fil.ion.ucl.ac.uk/spm/software/spm8). The structural MR images were segmented into gray matter (GM), white matter and cerebrospinal fluid based on an adaptive Maximum A Posterior (MAP) technique [Rajapakse et al., 1997] that was implanted into the VBM8 program (http://dbm.neuro.uni-jena.de/vbm8/). After an initial affine registration of the GM concentration map into the Montreal Neurological Institute (MNI) space (http://www.mni.mcgill.ca/), the GM concentration images were nonlinearly warped using diffeomorphic anatomical registration using the exponentiated Lie algebra (DARTEL) technique and were resliced to a resolution of 1.5 mm^3. The GMV of each voxel was obtained by multiplying the GM concentration map using the nonlinear determinants and ignoring the linear components, which represents the normalized GMV in the absence of the confounding effect of variance induced by individual whole brain size. Finally, to compensate for residual between-subject anatomical differences, the GMV images were smoothed with a full-width at half-maximum (FWHM) kernel of 8 mm. After spatial preprocessing, the smoothed, normalized GMV maps were used for statistical analysis.

Preprocessing of Resting-State fMRI Data

Functional MRI data were analyzed using the Data Processing Assistant for Resting-State fMRI (DPARSFA) [Yan and Zang, 2010]. The first 10 volumes from each subject were discarded to allow the signal to reach equilibrium and to allow the participants to adapt to the scanning noise. The remaining 170 volumes were corrected for acquisition time delay between slices. Next, the head motion parameters were estimated, and each volume was realigned to the mean map of the whole volumes to correct for geometric displacements using a six-parameter rigid-body transformation. Five subjects were excluded from further analysis because they had maximum displacements in one or more of the orthogonal directions (x, y, z) of >3 mm or a maximum rotation (x, y, z) > 3.0°. The data were spatially normalized to the standard EPI template and re-sampled to 2 × 2 × 2 mm^3. The normalized data were smoothed using a 4 mm FWHM.

Independent Component Analysis

We performed independent component analysis (ICA) using the group ICA (GICA) of the fMRI toolbox (Stable and Consistent Group ICA of the fMRI Toolbox, version 1.2; http://www.nitrc.org/projects/cogicat/), which was

established for the fMRI data analysis. Recently, Zhang et al. found that in a multistage principal component analysis (PCA) reduction, which was adopted and implemented in GIFT and MELODIC, different subject concatenation orders produced variation in the GICA results. To achieve robust and accurate results, an improved algorithm, the subject-order independent group ICA (SOI-GICA) [Zhang et al., 2010], was implemented multiple times with randomized initial values and different subject orders. Next, the results were integrated to form the final output. The toolbox supports a GICA approach that first concatenates the individual data across time and subsequently computes the subject-specific components and time courses. The toolbox performed the analysis in three stages: (i) data reduction, (ii) application of the ICA algorithm, and (iii) back-reconstruction for each individual subject. In this study, we adopted the SOI-GICA and performed GICA 100 times to obtain 40 independent components (ICs). The SN was identified by visual inspection, as previously described [Seeley et al., 2007]. The individual-level components were obtained from back-reconstruction and were converted into z-scores, which reflect the degree to which the time series of a given voxel correlates with the mean time series of its belonging component. For each SN component, the z-score of each voxel was defined as the resting-state intranetwork FC.

Definition of the CEN and DMN Masks

Although the CEN and DMN can be extracted using ICA, components of these networks were largely dependent on the predefined number of components. In ICA analysis, the DMN was divided into two components. Although the resulting CEN components were similar to the description of previous studies using the ICA method [Roosendaal et al., 2010], they were different from the task-derived CEN [Christoff et al., 2009; Duan et al., 2012; Sridharan et al., 2008]. Compared with the ICA method, the region of interest (ROI)-based method has also been widely used to extract the two functional networks, and the resulting networks were highly consistent with those derived from cognitive tasks. Thus, we adopted a ROI-based method to extract the CEN and DMN. The definition of ROIs of the CEN and DMN was based on a previous task fMRI study [Duan et al., 2012]. Four ROIs of the CEN, including the left dorsolateral prefrontal cortex (DLPFC) (MNI coordinates: −48, 34, 34), the right DLPFC (MNI coordinates: 48, 40, 30), the left posterior parietal cortex (PPC) (MNI coordinates: −36, −44, 46), and the right PPC (MNI coordinates: 42, −42, 48), and three ROIs of the DMN, including the ventromedial prefrontal cortex (VMPFC) (MNI coordinates: −2, 54, −6), the left posterior cingulate cortex (PCC) (MNI coordinates: −6, −48, 32), and the right PCC (MNI coordinates: 10, −52, 28) were selected for network extraction. Next, the time series of the mean BOLD signal of a 10-mm radius sphere centered at

the peak coordinate of each ROI was extracted to calculate the FC with each voxel of the whole brain in the 75 HYC. Prior to the statistical analysis, the FC maps were transformed into z-values using the Fisher transformation to improve normality. We then performed conjunction analyses to identify brain areas that were positively correlated with all of the CEN or DMN ROIs. A family-wise error (FWE) method with a threshold of $P < 0.05$ was selected to correct for multiple comparisons. Finally, the spatial distributions of the CEN and DMN were extracted as the masks.

GMV and Intranetwork FC Analyses in the SN

Individual ICA component maps of all subjects, independent of group, were entered into a random-effect one-sample t-test. Considering that the relatively large sample size (149 subjects) would greatly improve the statistical significance, we used a strict threshold of $P < 0.05$ (FWE correction) and $t > 11$ to create a sample-specific SN mask that included only the core nodes of the SN. Because the voxel sizes of the structural and functional images were different, we consistently used a cluster size threshold of >1 cm^3 in all of the statistical analyses, which corresponded to 296 voxels in the structural images with a resolution of $1.5 \times 1.5 \times 1.5$ mm^3 and 125 in the functional images with a resolution of $2 \times 2 \times 2$ mm^3.

One-way analysis of variance (ANOVA) was used to test the GMV and FC difference across groups within the SN mask with gender as a nuisance covariate. Multiple comparisons were corrected using the false discovery rate (FDR) method with significance thresholds of $P < 0.01$. Next, the mean GMV and FC values of each 1 cm^3 ROI with the most statistical significance were extracted. A general linear model (GLM) was used to compare the ROI differences in the GMV and FC between the HYC and HOC and among the HOC, aMCI, and AD ($P < 0.05$, Bonferroni correction for all comparisons for the MRI measure). To exclude the atrophy effect on the FC comparisons, we also repeated the ROI-based analyses of FC with correction for regional atrophy. Next, we used Cohen's d [Parker and Hagan-Burke, 2007] to describe the effect size of each comparison. Cohen [Cohen, 1988] defined effect sizes as "small: $d < 0.5$," "medium: $0.5 < d < 0.8$," and "large: $d > 0.8$."

To determine the associations of the structural and functional changes of the SN with cognitive differences, we performed voxel-based partial correlation analyses between the MMSE and GMV, as well as between the MMSE and FCs within the SN in older people. Age, gender, and years of education were used as nuisance covariates. ROI-based correlations were also performed to verify the voxel-wise results. To exclude atrophy effect on the correlation analyses between the MMSE and intranetwork FC, we also repeated the ROI-based analyses, which controlled for the GMV of each ROI.

Internetwork FC Analyses

We selected the bilateral FICs as ROIs to calculate internetwork FCs with the CEN and DMN because the FICs are the most frequently reported hub nodes of the SN and exhibited significant changes in the GMV or intranetwork FC across older subject groups after the atrophy correction. The time series of the mean BOLD signal of the left and right FICs were extracted to calculate the FC with each voxel of whole brain. Prior to the statistical analysis, the FC maps were also transformed into z-values using a Fisher transformation method. A voxel-wise one-way ANOVA was also used to test for internetwork FC differences ($P < 0.05$, FWE correction) across groups with gender as a nuisance covariate within the CEN or DNM mask. Next, the mean FC values of each 1 cm^3 ROI with the most statistical significance were extracted to investigate the differences between each pair of the four groups ($P < 0.05$, Bonferroni correction). Finally, partial correlation coefficients between the FC of each ROI and the MMSE scores were tested controlling for age, gender, and years of education in the older groups.

Validation

In this study, we used an uneven sample size across groups (a large number of HYC relative to the other groups), which may have biased our results. To validate our results, we only included 35 gender-matched healthy younger controls (the sample size was equal to the AD group) and repeated the above analyses. Considering the effects of outliers on the correlation analyses, for each of the three groups (HOC, aMCI, and AD), we used a criterion of mean ± 2SD (standard deviation) for each MRI measure (GMV, internetwork FC, and internetwork FC) to exclude the outliers in the correlation analyses between the MMSE and these MRI measures. We repeated these correlation analyses.

RESULTS

Components of the SN

Components of the SN were identified using the SOI-GICA technique and included the dACC/MPFC, bilateral FICs and DLPFCs (Fig. 2A). The components and locations were consistent with previous descriptions of the SN [Habas et al., 2009; Seeley et al., 2007; Thomason et al., 2011; Weissman-Fogel et al., 2010]. The data are displayed on a surface map using CARET software [van Essen, 2005].

CEN and DMN Masks

The CEN and DMN masks were defined using ROI-based FC analyses in combination with conjunction analyses. The DMN included the bilateral MPFC, PCC, lateral parietal cortices, anterior temporal lobes, and hippocampi
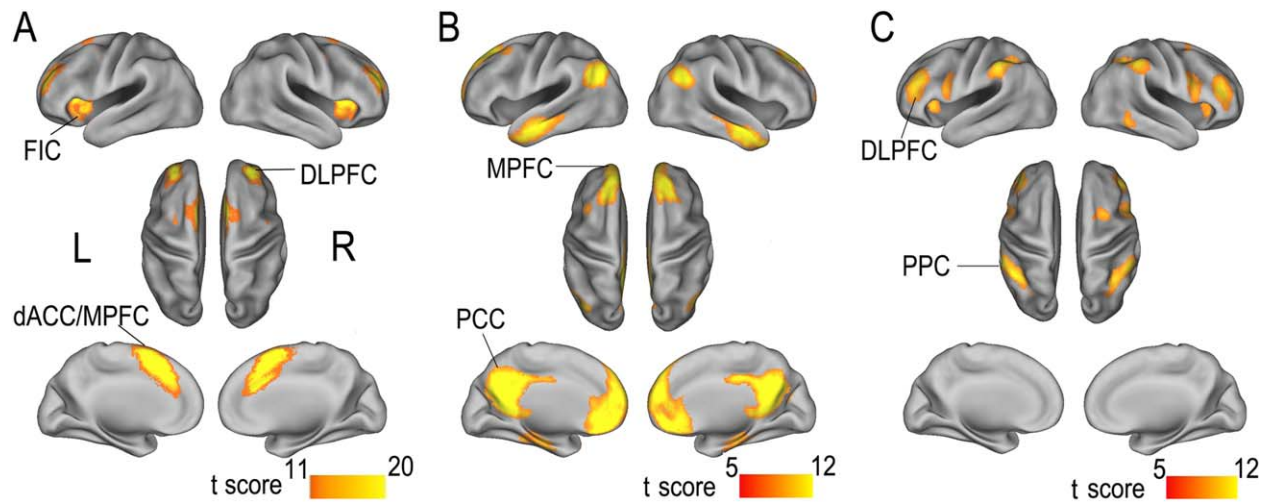
Figure 2.

Spatial maps of the SN (**A**), DMN (**B**), and CEN (**C**). The SN is identified using independent component analysis, whereas the CEN and DMN are identified using ROI-based functional connectivity analysis. Data are displayed on the lateral and medial surfaces of the left and right hemispheres of the surface map. Abbreviations: CEN, central executive network; dACC/MPFC, dorsal anterior cingulate cortex/medial prefrontal cortex; DLPFC, dorsolateral prefrontal cortex; DMN, default-mode network; FIC, frontoinsular cortex; L, left; MPFC, medial prefrontal cortex; PCC, posterior cingulate cortex; PPC, posterior parietal cortex; R, right; ROI, region of interest; SN, salience network. [Color figure can be viewed in the online issue, which is available at wileyonlinelibrary.com.]

(Fig. 2B), which was also consistent with previous descriptions [Greicius et al., 2003; Spreng et al., 2009; Sridharan et al., 2008]. The CEN mainly included the bilateral DLPFC and PPC (Fig. 2C), which was consistent with previous studies [Christoff et al., 2009; Koechlin and Summerfield, 2007; Sridharan et al., 2008].

GMV and Intranetwork FC Differences Within the SN Across Groups

A one-way ANOVA was used to identify brain regions within the SN mask that had GMV differences ($P < 0.01$, FDR corrected) across groups. Nearly all of the components of the SN showed significant GMV differences across groups, including the dACC/MPFC, bilateral FICs, and DLPFCs (Fig. 3A, Table II). We extracted an ROI of 1 cm^3 from each brain region with the most significant GMV difference. A post-hoc comparison of the GMV of each ROI was initially performed between the HYC and HOC groups ($P < 0.05$, corrected). Compared to the HYC, the HOC exhibited significant differences in the GMV in all five ROIs with a mean reduction of 20.1–32.3% (large effect size) (Fig. 3B, Table III). Next, the GMV of each ROI was compared among the HOC, aMCI, and AD groups ($P < 0.05$, corrected) (Fig. 3C, Table III). Compared to the HOC, patients with aMCI did not show any significant differences in the GMV in these ROIs. However, patients with AD demonstrated significant differences in the GMVs in four of the five ROIs with a mean reduction of 18.7–31.5%

(large effect size). AD patients exhibited a significant difference (23%) in the GMV in the ROI in the left FIC (large effect size), compared to patients with aMCI.

One-way ANOVA identified five brain regions that showed significant differences ($P < 0.01$, FDR corrected) in the intranetwork FC of the SN among the four groups (Fig. 4A, Table IV). We used the same method previously described for the VBM analysis to extract ROIs from these five brain regions, and the intranetwork FC strengths of the HYC and HOC groups are shown in Figure 4B. Compared with the HYC, the HOC exhibited significantly decreased (medium to large effect size) intranetwork FCs in the bilateral FICs, dACC, and left DLPFC and increased (medium effect size) intranetwork FC in the MPFC ($P < 0.05$, corrected). The intranetwork FC strengths of the HOC, aMCI, and AD groups are shown in Figure 4C. Compared with the HOC, patients with AD showed significantly decreased intranetwork FC in the right FIC and increased intranetwork FC in the MPFC ($P < 0.05$, corrected; medium effect size), whereas the left FIC showed a trend of decreased intranetwork FC ($P = 0.013$, uncorrected; small effect size). No significant differences in intranetwork FC were found between other combinations of groups using the same statistical threshold.

To exclude the effect of a GMV decrease on intranetwork FC, we repeated the ROI-based intranetwork FC comparisons with the GMV of each ROI as a covariate of no interest. After GMV correction, most of the intranetwork FC differences ($P < 0.05$, corrected) between groups remained,
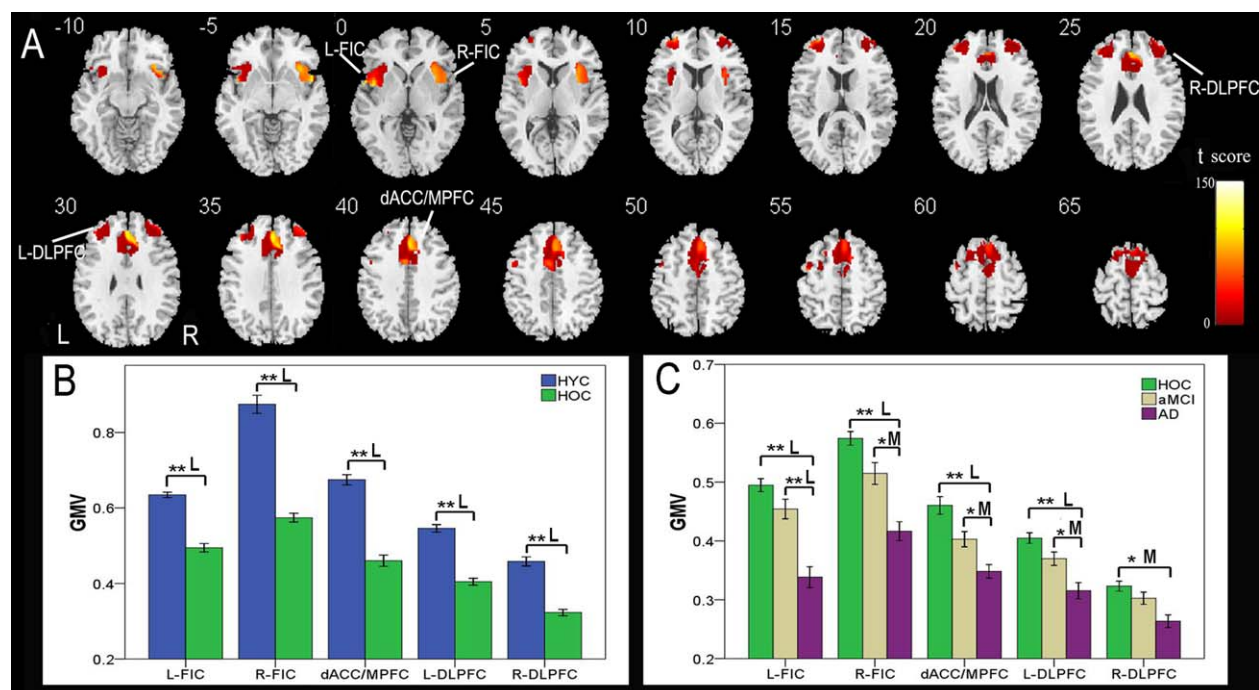
Figure 3.

GMV differences in the SN across groups. VBM analysis shows brain regions within the SN with GMV differences ($P < 0.01$, FDR corrected) across the four groups (**A**). Each ROI with the most statistical significance in the voxel-based analyses were then extracted. ROI analysis shows GMV differences in brain regions of the SN between the HYC and HOC (**B**) and among the HOC, aMCI, and AD (**C**). The x-axis represents the ROIs and the y-axis represents the GMV of each ROI. Error bars indicate the standard error of the mean. *$P < 0.05$, uncorrected; **$P < 0.05$, Bonferroni corrected. "S," "M," and "L" represent small, medium, and large effect sizes, respectively. Abbreviations: AD, Alzheimer's disease; aMCI, amnestic mild cognitive impairment; dACC/MPFC, dorsal anterior cingulate cortex/medial prefrontal cortex; DLPFC, dorsolateral prefrontal cortex; FDR, false discovery rate; FIC, frontoinsular cortex; GMV, gray matter volume; HYC, healthy younger control; HOC, healthy older control; L, left; R, right; ROI, region of interest; SN, salience network. [Color figure can be viewed in the online issue, which is available at wileyonlinelibrary.com.]

except for the differences in the MPFC between the HYC and HOC and between the HOC and AD (Fig. 4D,E).

Next, we investigated the overlap between brain regions with GMV differences and those with intranetwork FC differences in the SN by overlapping the two difference maps. We found that all of the brain regions with significant intranetwork FC differences in the SN in the older groups were located in regions that had significant differences in the GMV (Fig. 5).

Group Differences in Internetwork FC Between FICs and CEN

The bilateral FICs showed positive FC with the CEN. One-way ANOVA identified four brain regions of the CEN that showed significant differences ($P < 0.05$, FWE

TABLE II. Brain areas with significant differences in GMV across the four groups

Regions	BA	Cluster size (voxels)	Peak t-score	MNI coordination (x, y, z)
L-FIC	13	1,944	107.72	−54, 6, −2
R-FIC	13	1,712	95.17	36, 23, −8
dACC/MPFC	32/8	9,921	107.69	2, 35, 33
L-DLPFC	10	2,008	77.75	−29, 56, 14
R-DLPFC	10	1,915	56.39	33, 60, 11

BA, Brodmann's area; dACC/MPFC, dorsal anterior cingulate cortex/medial prefrontal cortex; GMV, gray matter volume; L-DLPFC, left dorsolateral prefrontal cortex; L-FIC, left frontoinsular cortex; MNI, Montreal Neurological Institute; R-DLPFC, right dorsolateral prefrontal cortex; R-FIC, right frontoinsular cortex.

GMV	HOC < HYC (%)	aMCI < HOC (%)	AD < aMCI (%)
Whole brain	12.3	3.1	14.9
SN	14.0	5.9	13.2
L-FIC	20.1	8.5	23.0
R-FIC	32.3	10.7	17.4
dACC/MPFC	30.5	12.6	12.8
L-DLPFC	24.2	9.0	13.5
R-DLPFC	27.6	6.9	11.8

AD, Alzheimer's disease; aMCI, amnestic mild cognitive impairment; dACC/MPFC, dorsal anterior cingulate cortex/ medial prefrontal cortex; GMV, gray matter volume; HOC, healthy older control; HYC, healthy younger control; L-DLPFC, left dorsolateral prefrontal cortex; L-FIC, left frontoinsular cortex; R-DLPFC, right dorsolateral prefrontal cortex; R-FIC, right frontoinsular cortex; SN, salience network.

corrected) in internetwork FC with the left FIC among the four groups (Fig. 6A, Table V). We used the same method previously described for the VBM analysis to extract ROIs from these four brain regions, and the internetwork FC strengths of the left FIC in the HYC and HOC groups are shown in Figure 6C. Compared to the HYC, the HOC exhibited significant differences in internetwork FC in the bilateral supramarginal gyrus (SMG), right middle frontal gyrus (MFG), and right inferior frontal gyrus (IFG) ($P <$ 0.05, corrected; medium to large effect size). The internetwork FC strengths between the left FIC and the CEN in the HOC, aMCI, and AD groups are shown in Figure 6D. Compared to the HOC, patients with aMCI and AD showed significant differences in internetwork FC with the right IFG ($P <$ 0.05, corrected; medium effect size), whereas the left SMG showed a trend towards a decreased internetwork FC ($P =$ 0.047, uncorrected; small effect size). No significant differences in internetwork FC were found in other comparisons under the same statistical threshold.

One-way ANOVA also identified four brain regions in the CEN that showed significant differences ($P <$ 0.05, FWE correction) in internetwork FC with the right FIC among the four groups (Fig. 7A, Table VI). Compared to the HYC, the HOC exhibited significant differences in internetwork FC in the bilateral MFGs and SMGs ($P <$ 0.05, corrected; medium to large effect size) (Fig. 7C). The internetwork FC strengths between the right FIC and the CEN in the HOC, aMCI, and AD groups are shown in Figure 7D. Compared to the HOC, patients with AD showed significant differences in internetwork FC in the right MFG and bilateral SMGs ($P <$ 0.05, corrected; medium to large effect size), whereas the left MFG showed a trend towards decreased internetwork FC ($P =$ 0.022, uncorrected; medium effect size). Patients with aMCI also showed a trend towards decreased internetwork FCs in the left ($P =$ 0.019, uncorrected; medium effect size) and

right ($P =$ 0.033, uncorrected; medium effect size) MFGs. AD patients exhibited a trend towards decreased internetwork FCs in the left SMG ($P =$ 0.021, uncorrected; medium effect size), compared to patients with aMCI. No significant differences in internetwork FC were found in other comparisons under the same statistical threshold.

## Group Differences in Internetwork FC Between FICs and DMN

The bilateral FICs showed negative FCs with the DMN. One-way ANOVA identified four brain regions of the DMN that showed significant differences ($P <$ 0.05, FWE correction) in internetwork FCs with the left FIC among the four groups (Fig. 6B). Compared to the HYC, the HOC exhibited significant differences in internetwork FCs in the MPFC, bilateral PCCs, and left angular gyrus (AG) ($P <$ 0.05, corrected; medium to large effect size) (Fig. 6C). The internetwork FC strengths between the left FIC and DMN in the HOC, aMCI, and AD groups are shown in Figure 6D. Compared to the HOC, patients with AD showed a significant difference in internetwork FC with the MPFC ($P <$ 0.05, corrected; medium effect size), whereas the left AG showed a trend towards decreased internetwork FC in AD ($P =$ 0.020, uncorrected; medium effect size) and aMCI patients ($P =$ 0.030, uncorrected; medium effect size). No significant differences in internetwork FC were found in other comparisons under the same statistical threshold.

One-way ANOVA identified four regions of the DMN that showed significant differences ($P <$ 0.05, FWE correction) in internetwork FC with the right FIC among the four groups (Fig. 7B). Compared to the HYC, the HOC exhibited significant differences in internetwork FC in the MPFC, bilateral PCCs, and left AG ($P <$ 0.05, corrected; medium to large effect size) (Fig. 7C). The internetwork FC strengths between the right FIC and DMN in the HOC, aMCI, and AD groups are shown in Figure 7D. Compared to the HOC, the left AG showed significant differences in internetwork FC in AD and aMCI patients ($P <$ 0.05, corrected; medium effect size), and the MPFC showed significant differences in internetwork FC in AD ($P <$ 0.05, corrected; medium effect size). Compared with aMCI patients, the left PCC showed a trend towards decreased internetwork FC in AD ($P =$ 0.020, uncorrected; medium effect size). No significant differences in internetwork FC were found in other comparisons under the same statistical threshold.

Correlations Between the GMV of the SN and MMSE in Older Subjects

It is important to know whether a reduction in the GMV in the SN is associated with cognitive decline in older subjects. Thus, we performed voxel-based partial correlation analyses between the MMSE and GMV within the SN in the three groups of older people with age, gender, and years of education as nuisance covariates. We found that
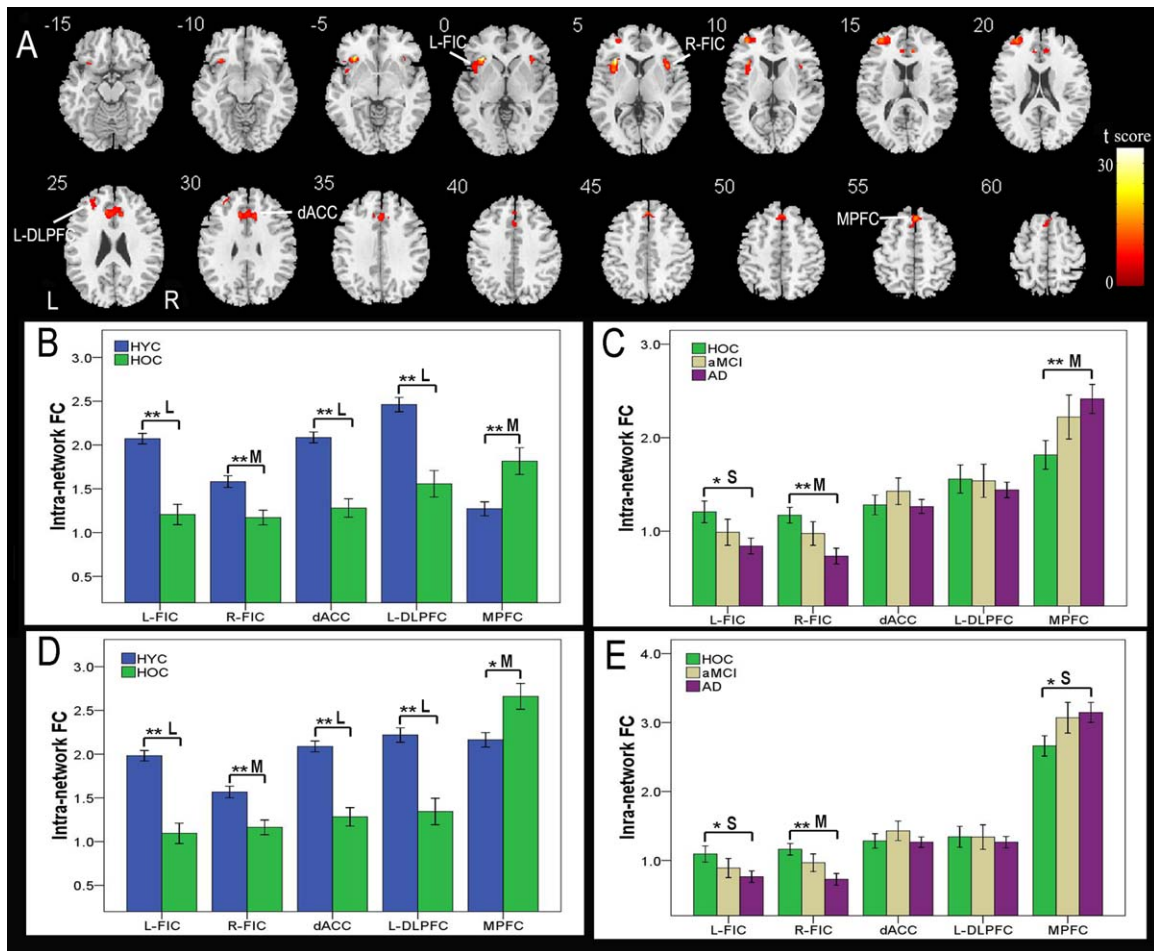
Figure 4.

Intranetwork FC differences in the SN across groups. Voxel-based analysis shows brain regions of the SN with intranetwork FC differences ($P < 0.01$, FDR corrected) across the four groups (**A**). Each ROI with the most statistical significance in the voxel-based analyses were then extracted. ROI analysis shows intranetwork FC differences in brain regions of the SN between the HYC and HOC (**B**) and among the HOC, aMCI, and AD (**C**). To exclude the effect of GMV decrease on the intranetwork FC, we repeated the ROI-based intranetwork FC comparisons using the GMV of each ROI as a covariate of no interest (**D**, **E**). The x-axis represents the ROIs and the y-axis represents the intranetwork FC of each ROI. Error bars indicate the stand-ard error of the mean. *$P < 0.05$, uncorrected; **$P < 0.05$, Bonferroni corrected. "S," "M," and "L" represent small, medium, and large effect sizes, respectively. Abbreviations: AD, Alzheimer's disease; aMCI, amnestic mild cognitive impairment; dACC, dorsal anterior cingulate cortex; DLPFC, dorsolateral prefrontal cortex; FC, functional connectivity; FDR, false discovery rate; FIC, frontoinsular cortex; HOC, healthy older control; HYC, healthy younger control; L, left; MPFC, medial prefrontal cortex; R, right; ROI, region of interest; SN, salience network. [Color figure can be viewed in the online issue, which is available at wileyonlinelibrary.com.]

the MMSE scores were positively correlated with the GMVs bilaterally in the FIC, DLPFC, and dACC/MPFC ($P < 0.01$, FDR corrected) (Fig. 8). We further extracted the regions with significant correlations as ROIs and calculated the partial correlation coefficients (*pr*) of these ROIs. We found significant correlations between the MMSE scores and the GMVs of these ROIs (Fig. 9).

Correlations Between Intranetwork FC of the SN and MMSE in Older Subjects

We performed voxel-based partial correlation analyses between the MMSE and the intranetwork FC of the SN in the three groups of older people with age, gender, and years of education as nuisance covariates. We found that

TABLE IV. Brain areas with significant differences in intranetwork FC across the four groups

Regions	BA	Cluster size (voxels)	Peak t-score	MNI coordination (x, y, z)
L-FIC	13	425	33.70	−34, 24, 6
R-FIC	13	137	15.02	38, 16, 6
dACC	32	481	13.44	10, 38, 16
L-DLPFC	10	364	16.62	−34, 52, 14
MPFC	8	217	15.93	0, 28, 54

BA, Brodmann's area; dACC, dorsal anterior cingulate cortex; FC, functional connectivity; L-DLPFC, left dorsolateral prefrontal cortex; L-FIC, left frontoinsular cortex; MNI, Montreal Neurological Institute; MPFC, medial prefrontal cortex; R-FIC, right frontoinsular cortex.

the intranetwork FC of the left FIC was positively correlated with the MMSE scores ($P < 0.05$, FDR corrected) (Fig. 10). We further extracted this region as an ROI and found significant correlations between the MMSE scores and the intranetwork FC of the left FIC with ($pr = 0.307$, $P = 0.010$) and without ($pr = 0.540$, $P < 0.001$) GMV correction (Fig. 11).

Correlations Between Internetwork FC of the SN and MMSE in Older Subjects

Each internetwork FC with a significant group difference was extracted and correlated with the MMSE scores
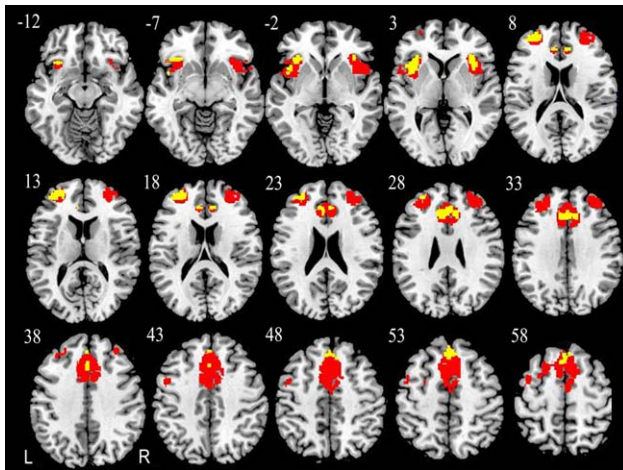
Figure 5.
Overlap between brain regions in the SN with GMV differences and those with intranetwork FC differences. Red indicates GMV differences and yellow represents intranetwork FC differences. Abbreviations: FC, functional connectivity; GMV, gray matter volume; L, left; R, right; SN, salience network. [Color figure can be viewed in the online issue, which is available at wileyonlinelibrary.com.]

using a partial correlation analysis controlling for age, gender, and years of education ($P < 0.05$). For the components of the CEN, the MMSE scores were positively correlated with the internetwork FCs between the left FIC and left SMG (Fig. 12) and between the right FIC and left MFG, right MFG, left SMG, and right SMG (Fig. 13). For the components of the DMN, the MMSE scores were negatively correlated with the internetwork FCs between the left FIC and MPFC and left AG (Fig. 12) as well as between the right FIC and left PCC, right PCC, and left AG (Fig. 13).

Validation

To avoid the effect of an uneven sample size across groups on our results, we selected 35 gender-matched healthy younger controls and repeated the above analyses. We found that the results were very similar to the above findings (see Part I of the Supporting Information). After using the criterion of mean ± 2SD to exclude outliers, we repeated the correlation analyses of the MMSE with the GMV, intranetwork FC, and internetwork FC. We found that most of the significant correlations remained except for the correlation between the right FIC and left MFG (see Part II of the Supporting Information)

DISCUSSION

In this study, we examined the associations of structural and functional deficits of the SN with normal aging and cognitive decline in aMCI and AD, which have not been previously described. Compared with healthy younger subjects, healthy older subjects showed substantial atrophy and intranetwork FC deficits in the SN and functional

TABLE V. Brain areas with significant differences in internetwork FC with the left FIC across the four groups

Regions	BA	Cluster size (voxels)	Peak t-score	MNI coordination (x, y, z)
R-MFG	10	320	22.26	40, 46, 20
R-IFG	44	161	20.42	58, 16, 24
L-SMG	40	164	20.51	−58, −32, 44
R-SMG	40	821	20.65	64, −40, 40
MPFC	11	2,222	39.53	0, 46, −22
L-PCC	31	453	24.67	−10, −62, 18
R-PCC	31	352	23.07	10, −58, 12
L-AG	39	150	17.77	−50, −62, 34

BA, Brodmann's area; FC, functional connectivity; FIC, frontoinsular cortex; L-AG, left angular gyrus; L-IFG, left inferior frontal gyrus; L-PCC, left posterior cingulate cortex; L-SMG, left supramarginal gyrus; MNI, Montreal Neurological Institute; MPFC, medial prefrontal cortex; R-MFG, right middle frontal gyrus; R-PCC, right posterior cingulate cortex; R-SMG, right supramarginal gyrus.
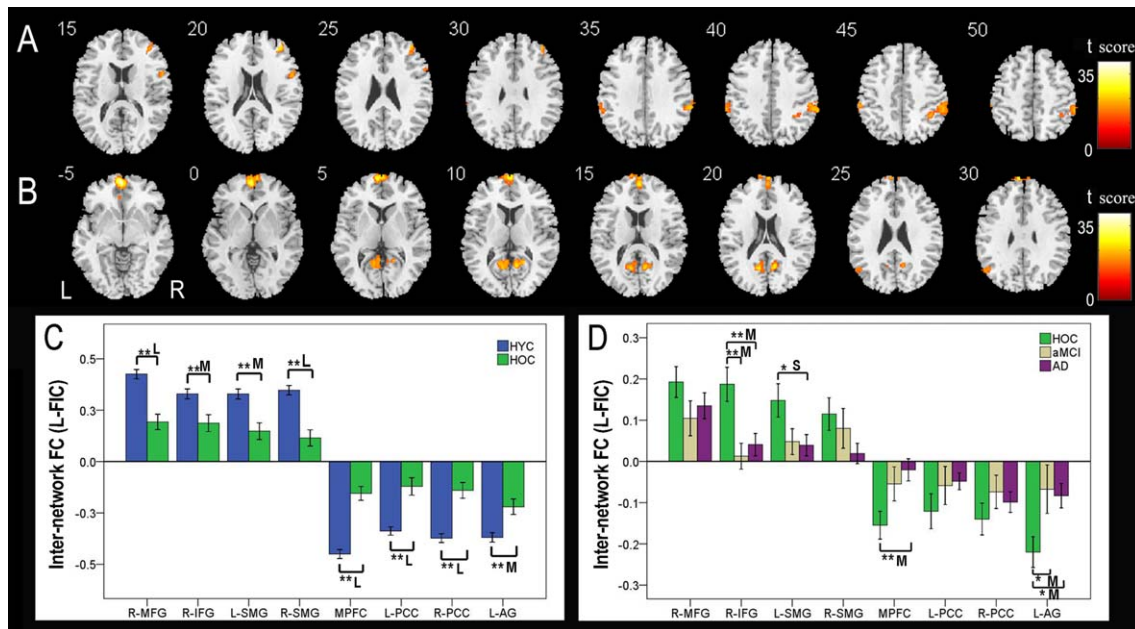
Figure 6.

Internetwork FC differences of the left FIC across groups. Voxel-based analysis shows brain regions of the CEN (**A**) and DMN (**B**) that have internetwork FC differences ($P < 0.05$, FWE corrected) with the left FIC across the four groups. Each ROI with the most statistical significance in the voxel-based analyses were then extracted. ROI analysis shows brain regions of the CEN and DMN between the HYC and HOC (**C**) and among the HOC, aMCI, and AD (**D**) that have internetwork FC differences with the left FIC across the four groups. The x-axis represents the ROIs and the y-axis represents the internetwork FC of each ROI. Error bars indicate the standard error of the mean. *$P < 0.05$, uncorrected; **$P < 0.05$, Bonferroni corrected. "S," "M," and "L" represent small, medium, and large effect sizes, respectively. Abbreviations: AD, Alzheimer's disease; AG, angular gyrus; aMCI, amnestic mild cognitive impairment; CEN, central executive network; dACC, dorsal anterior cingulate cortex; DLPFC, dorsolateral prefrontal cortex; DMN, default-mode network; FC, functional connectivity; FIC, frontoinsular cortex; FWE, family-wise error; HOC, healthy older control; HYC, healthy younger control; IFG, inferior frontal gyrus; L, left; MFG, middle frontal gyrus; MPFC, medial prefrontal cortex; PCC, posterior cingulate cortex; R, right; ROI, region of interest; SMG, supramarginal gyrus; SN, salience network. [Color figure can be viewed in the online issue, which is available at wileyonlinelibrary.com.]

disconnections between the core nodes (FICs) of the SN and the CEN and DMN, suggesting that structural and functional impairments of the SN occur in normal aging. Furthermore, our findings revealed that the structural and functional deficits in the bilateral FICs are associated with cognitive decline in elderly people.

Impaired SN in Normal Aging

The most important finding of this study was that the structural and functional impairments of the SN are present as a part of normal aging. Atrophy (20–32%) of several regions in the SN was significantly above the level of the whole brain (12%), and alterations in intra-network FC were present after atrophy correction, suggesting the presence of structural and functional impairments in the SN. The FICs serve to identify salient stimuli from the vast and continuous stream of various sensory inputs. The structural and functional

TABLE VI. Brain areas with significant differences in inter-network FC with the right FIC across the four groups

Regions	BA	Cluster size (voxels)	Peak t-score	MNI coordination (x, y, z)
L-MFG	10	429	35.81	−40, 44, 22
R-MFG	10	897	41.35	38, 50, 26
L-SMG	40	384	27.83	−62, −22, 28
R-SMG	40	781	31.22	62, −38, 40
MPFC	11	2,035	49.95	0, 46, −22
L-PCC	31		32.31	−12, −58, 20
R-PCC	31	1,285	34.99	8, −58, 12
L-AG	39	337	25.25	−56, −64, 32

BA, Brodmann's area; FC, functional connectivity; FIC, frontoinsular cortex; L-AG, left angular gyrus; L-MFG, left middle frontal gyrus; L-PCC, left posterior cingulate cortex; L-SMG, supramarginal gyrus; MNI, Montreal Neurological Institute; MPFC, medial prefrontal cortex; R-MFG, right middle frontal gyrus; R-PCC, right posterior cingulate cortex; R-SMG, right supramarginal gyrus.
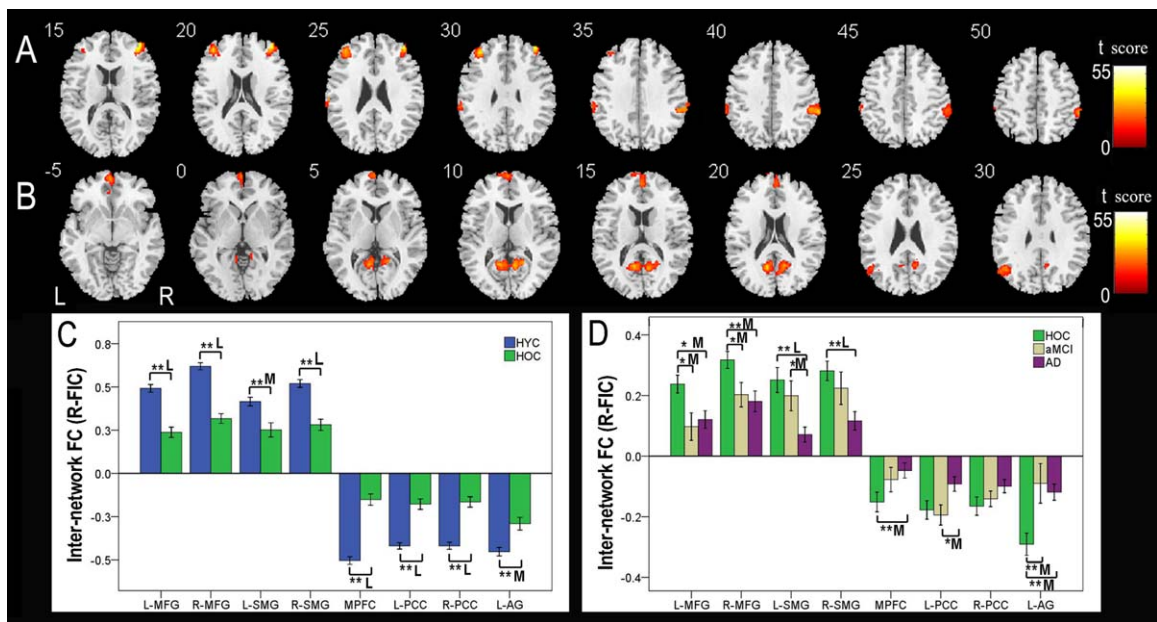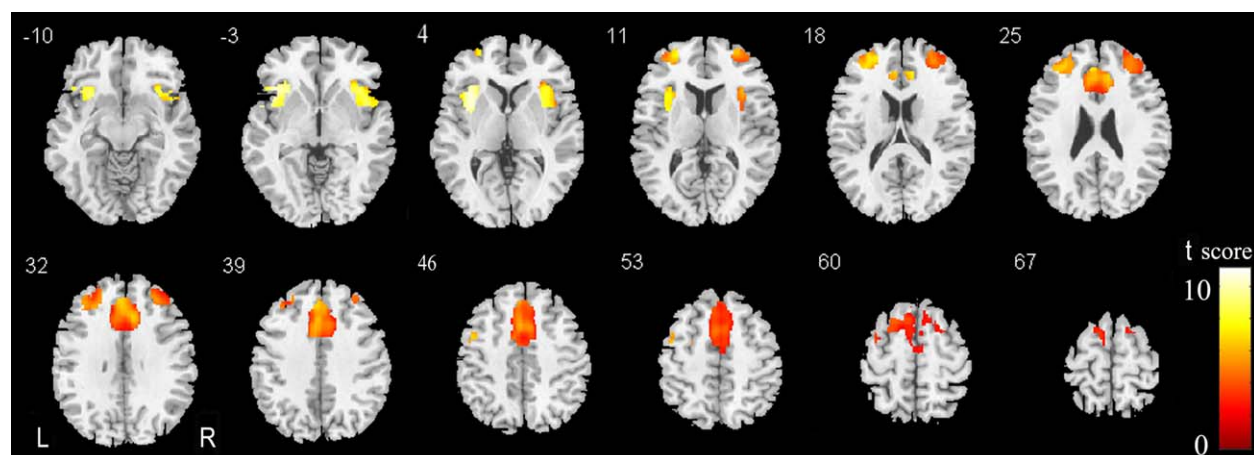
Figure 7.

Internetwork FC differences of the right FIC across groups. Voxel-based analysis shows brain regions of the CEN (**A**) and DMN (**B**) that have internetwork FC differences ($P < 0.05$, FWE corrected) with the right FIC across the four groups. Each ROI with the most statistical significance in the voxel-based analyses were then extracted. ROI analysis shows brain regions of the CEN and DMN between the HYC and HOC (**C**) and among the HOC, aMCI, and AD (**D**) that have internetwork FC differences with the right FIC across the four groups. The x-axis represents the ROIs, and the y-axis represents the internetwork FC of each ROI. Error bars indicate the standard error of the mean. *$P < 0.05$, uncorrected; **$P < 0.05$, Bonferroni corrected. "S," "M," and "L" represent small, medium, and large effect sizes, respectively. Abbreviations: AD, Alzheimer's disease; AG, angular gyrus; aMCI, amnestic mild cognitive impairment; CEN, central executive network; dACC, dorsal anterior cingulate cortex; DLPFC, dorsolateral prefrontal cortex; DMN, default-mode network; FC, functional connectivity; FIC, frontoinsular cortex; FWE, family-wise error; HOC, healthy older control; HYC, healthy younger control; IFG, inferior frontal gyrus; L, left; MFG, middle frontal gyrus; MPFC, medial prefrontal cortex; PCC, posterior cingulate cortex; R, right; ROI, region of interest; SMG, supramarginal gyrus; SN, salience network. [Color figure can be viewed in the online issue, which is available at wileyonlinelibrary.com.]

impairments of the FICs in healthy older people will impair the ability to identify salient stimuli, which has been confirmed by previous findings of declines in perception capacity [Cullum et al., 2000], attraction to novelty [Blau, 1973; Langer, 1989], responsiveness to novelty, and altered processing of rare targets in older subjects [Fabiani and Friedman, 1995; Walhovd and Fjell, 2001]. Consistent with our findings, the bilateral FICs have frequently been reported to have significantly decreased GMV in normal aging [Good et al., 2001; Ohnishi et al., 2001]. In addition, our finding of decreased intranetwork FC within the SN was consistent with the finding that reduced intranetwork FC within the SN is an important feature for distinguishing subjects of different ages [Meier et al., 2012; Onoda et al., 2012].

The dorsal ACC has been reported to be involved in a variety of cognitive functions, such as attention control [Silton et al., 2010], conflict monitoring [Kerns et al., 2004], error monitoring and detection [Gehring and Knight, 2000;

Menon et al., 2001], and response selection [Turken and Swick, 1999]. Most of these functions, including a decline of attention control [Bolton and Staines, 2012; Coubard et al., 2011], impaired performance on error monitoring [Pietrzak et al., 2007], and a decline in executive function [de Luca et al., 2003; El Haj and Allain, 2012; Treitz et al., 2007], have been reported to be impaired in normal aging. The significant differences in the GMV and intranetwork FC in the dorsal ACC suggest structural and functional impairment of this structure in older people, which may underlie the impaired functions of the dorsal ACC. Significantly atrophied GMV has also been reported in the dACC in healthy older subjects relative to younger subjects [Good et al., 2001; Giorgio et al., 2010; Hutton et al., 2009]. Furthermore, the reduced intranetwork FC within the SN is a hallmark of normal aging [Meier et al., 2012; Onoda et al., 2012]. Similarly, the significantly decreased GMV and intranetwork FC in the DLPFC in older people, found in our study and in other studies [Meier et al., 2012;

Figure 8.
Brain regions of the SN where the GMV is positively correlated with the MMSE scores. Abbreviations: GMV, gray matter volume; L, left; MMSE, Mini-Mental State Examination; R, right; SN, salience network. [Color figure can be viewed in the online issue, which is available at wileyonlinelibrary.com.]

Giorgio et al., 2010; Hutton et al., 2009], may contribute to the impaired cognitive functions in older people [MacDonald, 2000; Sharp et al., 2006]. These functions include working memory, executive control, and attention, which are controlled by the DLPFC [Curtis and D'Esposito, 2003; Sharp et al., 2006].

The right FIC of the SN has been shown to initiate control signals that enable a switch between the CEN and DMN in response to cognitive demands [Sridharan et al., 2008], which is important for cognitive function. The structural and functional impairments of the right FIC in healthy older people will result in an alteration in the capacity to switch between the CEN and DMN and will inevitably result in cognitive decline. As expected, compared with healthy younger subjects, healthy older subjects showed significantly weakened positive internetwork FCs between the right FIC and CEN as well as significantly weakened negative internetwork FCs between the right FIC and DMN. These findings suggested that the internetwork functional disconnection between the right FIC and the CEN and DMN is a hallmark of normal aging that may be associated with cognitive decline in elderly people. Interestingly, we also found weakened internetwork FCs between the left FIC and the CEN and DMN in healthy older subjects, which suggests that the left FIC may play a similar role to the right FIC in switching between the CEN and DMN. However, this speculation should be validated in future studies.

In addition to the decreased intranetwork FC in the SN of older people, we also found increased intranetwork FC in the MPFC in normal aging, and more significantly, in AD, although the GMV in this brain region was decreased. Increased SN connectivity has been reported in patients with AD [Zhou et al., 2010], which is partly consistent

with the results of our study. However, the functional implication of these findings remains unclear. Some authors [Zhou et al., 2010] attributed this finding to heightened emotional sensitivity and emotional sensitization, including factors such as irritability and anxiety [Benoit et al., 1999; Mega et al., 1996]. Alternatively, the increased SN connectivity in older people might reflect compensation for impairments of the SN [Agosta et al., 2011], which is supported in part by the cognitive reserve phenomenon that enables some patients to perform better than others despite equivalent pathological burdens [Stern, 2006]. Thus, older people may compensate for their impaired brain function by increasing the intranetwork FC of the SN to retain at least part of their cognitive performance.

Impaired SN in aMCI/AD

Compared with healthy older subjects, most of the brain regions within the SN showed reduced GMV in AD, suggesting substantial atrophy of the SN. All regions in the SN exhibited significant atrophy in the GMV in AD and significant correlations between the GMV and MMSE scores in older subjects, indicating that the SN is associated with AD impairment and cognitive decline in older people. In the intranetwork FC analyses, the bilateral FICs showed significant differences in the intranetwork FCs between the AD and HOC subjects and the left FIC exhibited a significant correlation between intranetwork FC and MMSE scores in older subjects, suggesting that the FICs may be associated with AD impairment and cognitive decline in older people. As previously discussed, the FICs serve to identify salient stimuli from different types of sensory modalities [Cauda et al., 2011; Kurth, 2010]. Further
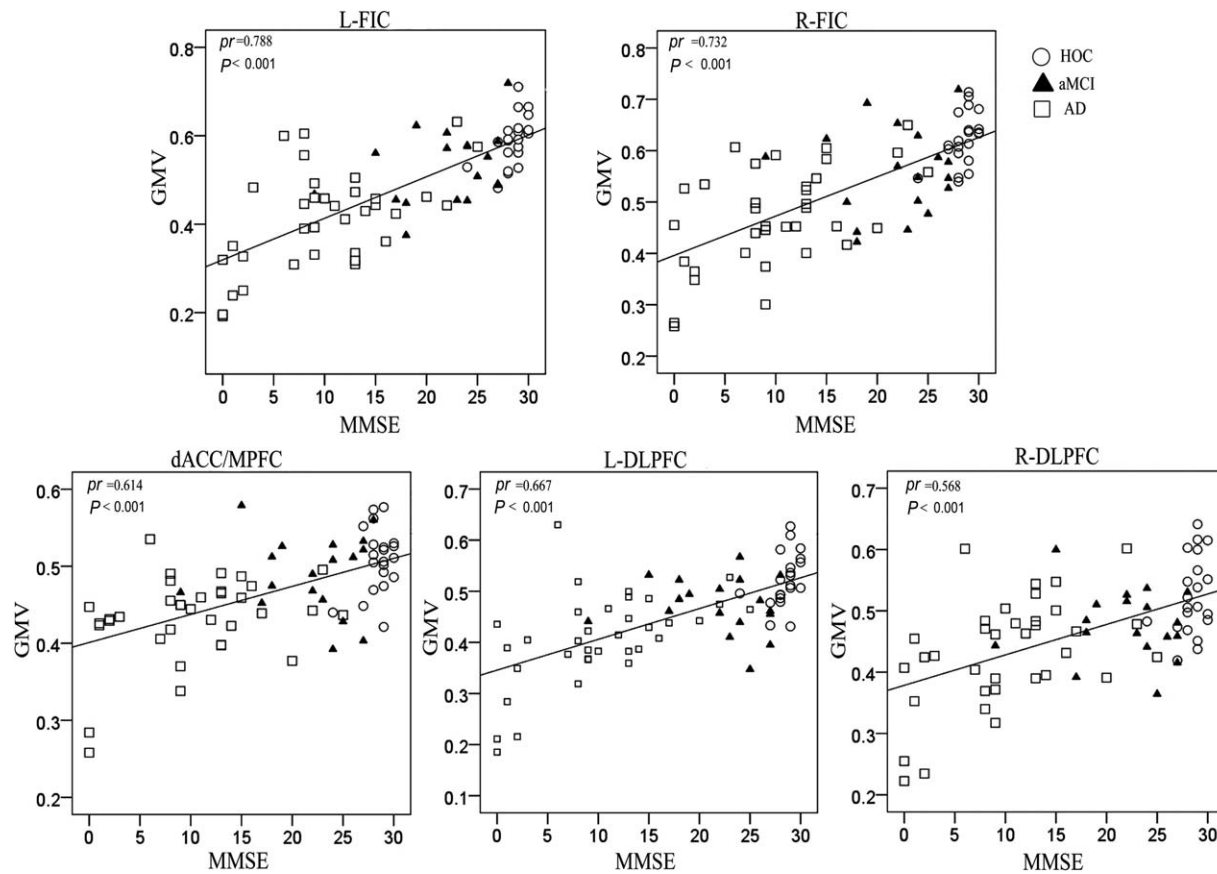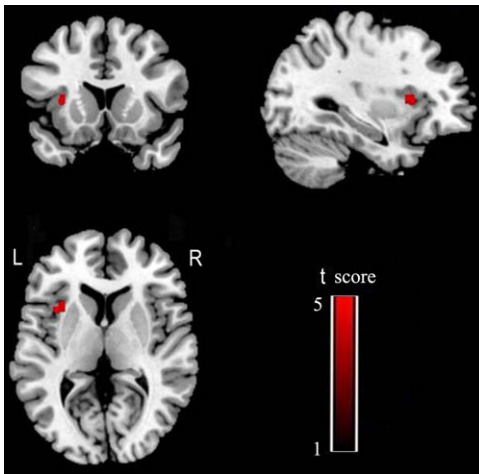
Figure 9.

Scatter plots of the GMVs of the SN regions versus MMSE scores. Abbreviations: AD, Alzheimer's disease; aMCI, amnestic mild cognitive impairment; dACC/MPFC, dorsal anterior cingulate cortex/medial prefrontal cortex; DLPFC, dorsolateral prefrontal cortex; FIC, frontoinsular cortex; GMV, gray matter volume; HOC, healthy older control; L, left; MMSE, Mini-Mental State Examination; pr, partial correlation coefficients; R, right; SN, salience network.

structural and functional impairments of the FICs in AD may weakened the capacity to identify salient stimuli [Blennow et al., 2006; Brier et al., 2012], which may result in an impairment of cognitive function. Furthermore, identification of salient stimuli is important for other higher functions, such as social-emotional information processing, which is severely impaired in patients with behavioral variant frontotemporal dementia, who also showed significantly impaired SN [Zhou et al., 2010].

The right FIC has been shown to initiate control signals that enable a switch between the CEN and DMN in response to cognitive demands [Sridharan et al., 2008]. The CEN and DMN have been frequently reported to be impaired in AD [Brier et al., 2012, Rombouts et al., 2005; Greicius, 2004; Jones et al., 2011; Sorg et al., 2007]. A recent study showed that the structural integrity of the SN is necessary for the efficient regulation of activity in the DMN and that a failure of this regulation results in inefficient

cognitive control [Bonnelle et al., 2012]. Thus, structural and functional impairments in the right FIC may be further associated with a deterioration of cognitive function in AD via a failure to efficiently switch between the CEN and DMN. This hypothesis is supported by the internetwork FC analysis, in which a weakened positive internetwork FC between the right FIC and CEN and a weakened negative internetwork FC between the right FIC and DMN in patients with AD compared to healthy older subjects was observed. Moreover, the significant correlations between the internetwork FCs and cognitive decline in elderly people also indicated an association between the disconnection of the SN with the CEN and DMN and cognitive decline.

As a transitional stage, aMCI is a syndrome defined by cognitive decline that is greater than expected for age and education level, but that does not notably interfere with the activities of daily living. Our study showed that most

Figure 10.

Brain regions of the SN whose intranetwork FCs are positively correlated with the MMSE scores. Abbreviations: FC, functional connectivity; L, left; MMSE, Mini-Mental State Examination; R, right; SN, salience network. [Color figure can be viewed in the online issue, which is available at wileyonlinelibrary.com.]
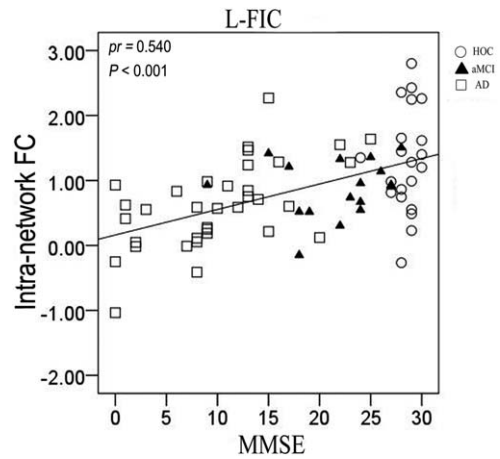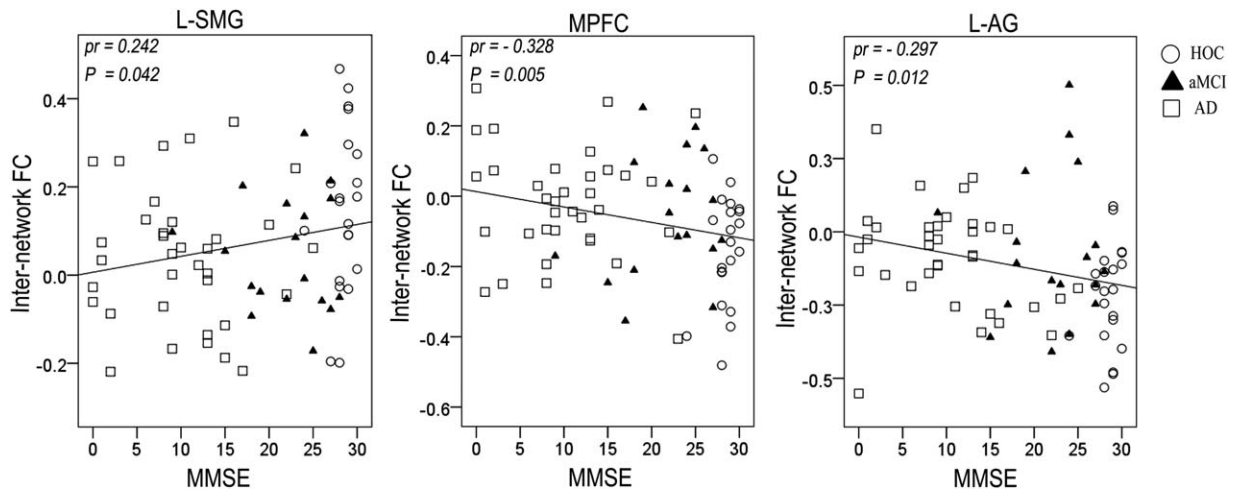

Figure 11.

Scatter plots of the intranetwork FCs of the SN regions versus MMSE scores. Abbreviations: AD, Alzheimer's disease; aMCI, amnestic mild cognitive impairment; FC, functional connectivity; HOC, healthy older control; L-FIC, left frontoinsular cortex; MMSE, Mini-Mental State Examination; pr, partial correlation coefficients.

of the structural and functional indices of aMCI fell between the HOC and AD groups, supporting aMCI as a transitional stage to AD [Celone et al., 2006]. Previous results of task-related fMRI in aMCI indicated that functional connectivity was already impaired in the prodromal stages of AD [Dannhauser et al., 2005; Dickerson et al., 2005]. Beyond the DMN, aMCI is associated with altera-

tions in large-scale functional brain networks, such as the SN [Liang et al., 2012; Xie et al., 2012]. In this study, we found that patients with aMCI and the HOC showed similar GMV in the SN, suggesting that cortical atrophy was not the critical factor for the difference in memory function between the two groups. However, significant differences (medium to large effect size) in the GMV of the SN

Figure 12.

Scatter plots of internetwork FCs of the left FIC versus MMSE scores. Abbreviations: AD, Alzheimer's disease; aMCI, amnestic mild cognitive impairment; FC, functional connectivity; FIC, frontoinsular cortex; HOC, healthy older control; L-AG, left angular gyrus; L-PCC, left posterior cingulate cortex; MMSE, Mini-Mental State Examination; MPFC, medial prefrontal cortex; pr, partial correlation coefficients.
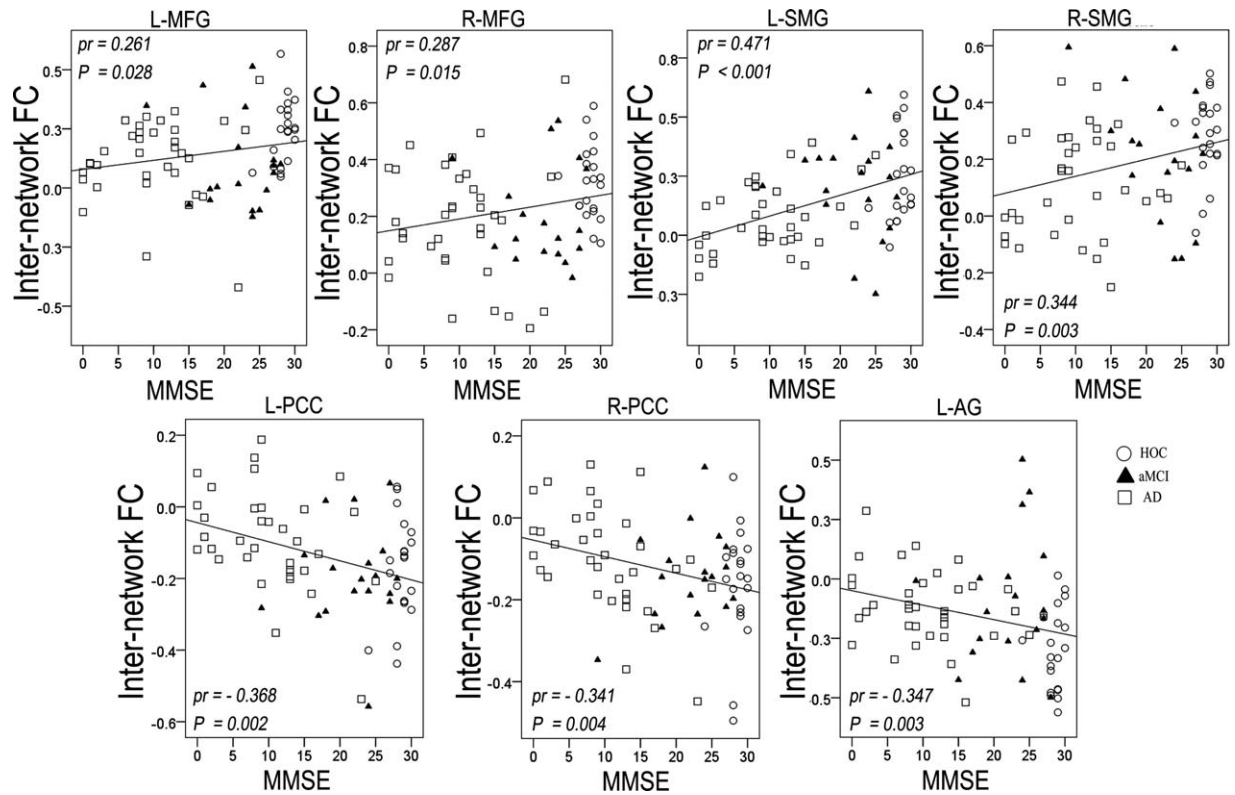
Figure 13.

Scatter plots of internetwork FCs of the right FIC versus MMSE scores. Abbreviations: AD, Alzheimer's disease; aMCI, amnestic mild cognitive impairment; FC, functional connectivity; FIC, frontoinsular cortex; HOC, healthy older control; L-AG, left angular gyrus; L-MFG, left middle frontal gyrus; L-PCC, left posterior cingulate cortex; L-SMG, left supramarginal gyrus; MMSE, Mini-Mental State Examination; MPFC, medial prefrontal cortex; pr, partial correlation coefficients; R-PCC, right posterior cingulate cortex; R-SMG, right supramarginal gyrus.

between the aMCI and AD may be associated with cognitive decline in AD. The lack of significant differences in the intranetwork FCs of the SN between the HOC and aMCI and between the aMCI and AD suggested that these measures could not be used as biomarkers for early diagnosis of AD. Compared with the HOC, the internetwork FCs of the left FIC with the right IFG and left AG and the internetwork FCs of the right FIC with the bilateral MFGs and left AG were significantly decreased (medium effect size) in the aMCI group, suggesting that these measures may be regarded as biomarkers of aMCI. Significant differences (medium effect size) in the internetwork FCs of the right FIC with the left SMG and PCC between the aMCI and AD may be associated with cognitive decline in AD.

Limitations

There were several limitations in this study. One limitation was the ceiling and floor effects on the MMSE in the healthy older controls and in the AD patients, respectively. The MMSE is also limited in terms of its sensitivity to high and low levels of cognitive functioning. More elaborate and accurate cognitive scales should be included in future studies. In addition, our current study was limited by the relatively small number of available samples, particularly in the middle-aged healthy control groups. Further studies using a larger sample size and more matched groups should be performed to validate our findings. Finally, because the uneven sample size across groups may have affected our results, we selected 35 gender-matched healthy younger controls and repeated the analyses and found similar results. In a future study, a more reasonable experimental design should be adopted.

CONCLUSION

We reported several novel findings: (1) both the structural and functional organization of the SN are impaired in AD/MCI and occur as early as in normal aging; (2) the structural and functional deficits in the FICs are important contributors to cognitive differences in older people; and

(3) the internetwork disconnection between the SN and the CEN and DMN occurs during normal aging and is associated with cognitive decline in elderly people. These findings improve our understanding of the association between the SN and normal aging and AD/MCI.

REFERENCES

Agosta F, Pievani M, Geroldi C, Copetti M, Frisoni GB, Filippi M (2011): Resting state fMRI in Alzheimer's disease: Beyond the default mode network. Neurobiol Aging 33:1564–1578.

Allman JM, Watson KK, Tetreault NA, Hakeem AY (2005): Intuition and autism: A possible role for Von Economo neurons. Trends Cogn Sci 9:367–373.

Andrews-Hanna JR, Snyder AZ, Vincent JL, Lustig C, Head D, Raichle ME Buckner RL (2007): Disruption of large-scale brain systems in advanced aging. Neuron 56:924–935.

Benoit M, Dygai I, Migneco O, Robert PH, Bertogliati C, Darcourt J, Benoliel J, Aubin-Brunet V, Pringuey D (1999): Behavioral and psychological symptoms in Alzheimer's disease. Relation between apathy and regional cerebral perfusion. Dement Geriatr Cogn Disord 10:511–517.

Binnewijzend MA, Schoonheim MM, Sanz-Arigita E, Wink AM, van der Flier WM, Tolboom N, Adriaanse SM, Damoiseaux JS, Scheltens P, van Berckel BN, Barkhof F (2011): Resting-state fMRI changes in Alzheimer's disease and mild cognitive impairment. Neurobiol Aging 33:2018–2028.

Blau Z (1973): Old Age in a Changing Society. New York: New Viewpoints.

Blennow K, de Leon MJ, Zetterberg H (2006): Alzheimer's disease. Lancet 368:387–403.

Bolton DA, Staines WR (2012): Age-related loss in attention-based modulation of tactile stimuli at early stages of somatosensory processing. Neuropsychologia 50:1502–1513.

Bonnelle V, Ham TE, Leech R, Kinnunen KM, Mehta MA, Greenwood RJ, Sharp DJ (2012): Salience network integrity predicts default mode network function after traumatic brain injury. Proc Natl Acad Sci USA 109:4690–4695.

Brier MR, Thomas JB, Snyder AZ, Benzinger TL, Zhang D, Raichle ME, Holtzman DM, Morris JC, Ances BM (2012): Loss of intranetwork and internetwork resting state functional connections with Alzheimer's disease progression. J Neurosci 32: 8890–8899.

Cauda F, D'Agata F, Sacco K, Duca S, Geminiani G, Vercelli A (2011): Functional connectivity of the insula in the resting brain. Neuroimage 55:8–23.

Celone KA, Calhoun VD, Dickerson BC, Atri A, Chua EF, Miller SL, DePeau K, Rentz DM, Selkoe DJ, Blacker D, Albert MS, Sperling RA (2006): Alterations in memory networks in mild cognitive impairment and Alzheimer's disease: An independent component analysis. J Neurosci 26:10222–10231.

Christoff K, Gordon AM, Smallwood J, Smith R, Schooler JW (2009): Experience sampling during fMRI reveals default network and executive system contributions to mind wandering. Proc Natl Acad Sci USA 106:8719–8724.

Cohen, J. 1988. Statistical Power Analysis for the Behavioral Sciences, 2nd ed. Hillsdale, NJ: Lawrence Erlbaum Associates, 567 p.

Coubard OA, Ferrufino L, Boura M, Gripon A, Renaud M, Bherer L (2011): Attentional control in normal aging and Alzheimer's disease. Neuropsychology 25:353–367.

Cullum S, Huppert FA, McGee M, Dening T, Ahmed A, Paykel ES, Brayne C (2000): Decline across different domains of cognitive function in normal ageing: Results of a longitudinal population-based study using CAMCOG. Int J Geriatr Psychiatry 15:853–862.

Curtis CE, D'Esposito M (2003): Persistent activity in the prefrontal cortex during working memory. Trends Cogn Sci 7: 415–423.

Damoiseaux JS, Rombouts SA, Barkhof F, Scheltens P, Stam CJ, Smith SM, Beckmann CF (2006): Consistent resting-state networks across healthy subjects. Proc Natl Acad Sci USA 103: 13848–13853.

Dannhauser TM, Walker Z, Stevens T, Lee L, Seal M, Shergill SS (2005): The functional anatomy of divided attention in amnestic mild cognitive impairment. Brain 128:1418–1427.

de Luca CR, Wood SJ, Anderson V, Buchanan JA, Proffitt TM, Mahony K, Pantelis C (2003): Normative data from the CANTAB. I: Development of executive function over the lifespan. J Clin Exp Neuropsychol 25:242–254.

Dickerson BC, Salat DH, Greve DN, Chua EF, Rand-Giovannetti E, Rentz DM, Bertram L, Mullin K, Tanzi RE, Blacker D, Albert MS, Sperling RA (2005): Increased hippocampal activation in mild cognitive impairment compared to normal aging and AD. Neurology 65:404–411.

Duan X, Liao W, Liang D, Qiu L, Gao Q, Liu C, Gong Q, Chen H (2012): Large-scale brain networks in board game experts: Insights from a domain-related task and task-free resting state. PloS one 7:e32532.

El Haj M, Allain P (2012): Relationship between source monitoring in episodic memory and executive function in normal aging. Geriatr Psychol Neuropsychiatr Vieil 10:197–205.

Fabiani M, Friedman D (1995): Changes in brain activity patterns in aging: The novelty oddball. Psychophysiology 32:579–594.

Fox MD, Snyder AZ, Vincent JL, Corbetta M, van Essen DC, Raichle ME (2005): The human brain is intrinsically organized into dynamic, anticorrelated functional networks. Proc Natl Acad Sci USA 102:9673–9678.

Gehring WJ, Knight RT (2000): Prefrontal-cingulate interactions in action monitoring. Nat Neurosci 3:516–520.

Giorgio A, Santelli L, Tomassini V, Bosnell R, Smith S, de Stefano N, Johansen-Berg H (2010): Age-related changes in grey and white matter structure throughout adulthood. Neuroimage 51: 943–951.

Good CD, Johnsrude IS, Ashburner J, Henson RN, Friston KJ, Frackowiak RS (2001): A voxel-based morphometric study of ageing in 465 normal adult human brains. Neuroimage 14: 21–36.

Greicius MD (2004): Default-mode network activity distinguishes Alzheimer's disease from healthy aging: Evidence from functional MRI. Proc Natl Acad Sci USA 101:4637–4642.

Greicius MD, Menon V (2004): Default-mode activity during a passive sensory task: Uncoupled from deactivation but impacting activation. J Cogn Neurosci 16:1484–1492.

Greicius MD, Krasnow B, Reiss AL, Menon V (2003): Functional connectivity in the resting brain: A network analysis of the default mode hypothesis. Proc Natl Acad Sci USA 100:253–258.

Habas C, Kamdar N, Nguyen D, Prater K, Beckmann CF, Menon V, Greicius MD (2009): Distinct cerebellar contributions to intrinsic connectivity networks. J Neurosci 29:8586–8594.

Hutton C, Draganski B, Ashburner J, Weiskopf N (2009): A comparison between voxel-based cortical thickness and voxel-based morphometry in normal aging. Neuroimage 48:371–380.

Jones DT, Machulda MM, Vemuri P, McDade EM, Zeng G, Senjem ML, Gunter JL, Przybelski SA, Avula RT, Knopman DS, Boeve BF, Petersen RC, Jack CR, Jr (2011): Age-related changes in the default mode network are more advanced in Alzheimer disease. Neurology 77:1524–1531.

Kerns JG, Cohen JD, MacDonald AW, III, Cho RY, Stenger VA, Carter CS (2004): Anterior cingulate conflict monitoring and adjustments in control. Science 303:1023–1026.

Koechlin E, Summerfield C (2007): An information theoretical approach to prefrontal executive function. Trends Cogn Sci 11:229–235.

Kurth F, Zilles K, Fox PT, Laird AR, Eickhoff SB (2010): A link between the systems: Functional differentiation and integration within the human insula revealed by meta-analysis. Brain Struct Funct 214:519–534.

Langer E (1989): Mindfulness. Reading, MA: Addison-Wesley Publishing Co.

Li R, Wu X, Chen K, Fleisher AS, Reiman EM, Yao L (2013): Alterations of directional connectivity among resting-state networks in Alzheimer disease. AJNR Am J Neuroradiol 34:340–345.

Liang P, Wang Z, Yang Y, Li K (2012): Three subsystems of the inferior parietal cortex are differently affected in mild cognitive impairment. J Alzheimers Dis 30:475–487.

MacDonald AW (2000): Dissociating the role of the dorsolateral prefrontal and anterior cingulate cortex in cognitive control. Science. 288:1835–1838.

McKhann G, Drachman D, Folstein M, Katzman R, Price D, Stadlan EM (1984): Clinical diagnosis of Alzheimer's disease: Report of the NINCDS-ADRDA Work Group under the auspices of Department of Health and Human Services Task Force on Alzheimer's Disease. Neurology 34:939–944.

Mega MS, Cummings JL, Fiorello T, Gornbein J (1996): The spectrum of behavioral changes in Alzheimer's disease. Neurology 46:130–135.

Meier TB, Desphande AS, Vergun S, Nair VA, Song J, Biswal BB, Meyerand ME, Birn RM, Prabhakaran V (2012): Support vector machine classification and characterization of age-related reorganization of functional brain networks. Neuroimage 60:601–613.

Menon V, Uddin LQ (2010): Saliency, switching, attention and control: A network model of insula function. Brain Struct Funct 214:655–667.

Menon V, Adleman NE, White CD, Glover GH, Reiss AL (2001): Error-related brain activation during a Go/NoGo response inhibition task. Hum Brain Mapp 12:131–143.

Morris JC (1993): The Clinical Dementia Rating (CDR): Current version and scoring rules. Neurology 43:2412–2414.

Ohnishi T, Matsuda H, Tabira T, Asada T, Uno M (2001): Changes in brain morphology in Alzheimer disease and normal aging: Is Alzheimer disease an exaggerated aging process? AJNR Am J Neuroradiol 22:1680–1685.

Onoda K, Ishihara M, Yamaguchi S (2012): Decreased functional connectivity by aging is associated with cognitive decline. J Cogn Neurosci 24:2186–2198.

Parker RI, Hagan-Burke S. (2007). Useful effect size interpretation for single case research. Behav Ther England 38:95–105.

Petersen RC, Stevens JC, Ganguli M, Tangalos EG, Cummings JL, DeKosky ST (2001): Practice parameter: Early detection of dementia: Mild cognitive impairment (an evidence-based review). Report of the Quality Standards Subcommittee of the American Academy of Neurology. Neurology 56:1133–1142.

Pietrzak RH, Cohen H, Snyder PJ (2007): Spatial learning efficiency and error monitoring in normal aging: An investigation using a novel hidden maze learning test. Arch Clin Neuropsychol 22:235–245.

Raichle ME, MacLeod AM, Snyder AZ, Powers WJ, Gusnard DA, Shulman GL (2001): A default mode of brain function. Proc Natl Acad Sci USA 98:676–682.

Rajapakse JC, Giedd JN, Rapoport JL (1997): Statistical approach to segmentation of single-channel cerebral MR images. IEEE Trans Med Imaging 16:176–186.

Rombouts SA, Barkhof F, Goekoop R, Stam CJ, Scheltens P (2005): Altered resting state networks in mild cognitive impairment and mild Alzheimer's disease: An fMRI study. Hum Brain Mapp 26:231–239.

Roosendaal SD, Schoonheim MM, Hulst HE, Sanz-Arigita EJ, Smith SM, Geurts JJ, Barkhof F (2010): Resting state networks change in clinically isolated syndrome. Brain 133 (Pt 6):1612–1621.

Seeley WW, Menon V, Schatzberg AF, Keller J, Glover GH, Kenna H, Reiss AL, Greicius MD (2007): Dissociable intrinsic connectivity networks for salience processing and executive control. J Neurosci 27:2349–2356.

Sharp DJ, Scott SK, Mehta MA, Wise RJ (2006): The neural correlates of declining performance with age: Evidence for age-related changes in cognitive control. Cereb Cortex 16:1739–1749.

Silton RL, Heller W, Towers DN, Engels AS, Spielberg JM, Edgar JC, Sass SM, Stewart JL, Sutton BP, Banich MT, Miller GA (2010): The time course of activity in dorsolateral prefrontal cortex and anterior cingulate cortex during top-down attentional control. Neuroimage 50:1292–1302.

Sorg C, Riedl V, Muhlau M, Calhoun VD, Eichele T, Laer L, Drzezga A, Förstl H, Kurz A, Zimmer C, Wohlschläger AM (2007): Selective changes of resting-state networks in individuals at risk for Alzheimer's disease. Proc Natl Acad Sci USA 104:18760–18765.

Spreng RN, Mar RA, Kim AS (2009): The common neural basis of autobiographical memory, prospection, navigation, theory of mind, and the default mode: A quantitative meta-analysis. J Cogn Neurosci 21:489–510.

Sridharan D, Levitin DJ, Menon V (2008): A critical role for the right fronto-insular cortex in switching between central-executive and default-mode networks. Proc Natl Acad Sci USA 105:12569–12574.

Stern Y (2006) Cognitive reserve and Alzheimer disease. Alzheimer Dis Assoc Disord 20:112–117.

Thomason ME, Hamilton JP, Gotlib IH (2011): Stress-induced activation of the HPA axis predicts connectivity between subgenual cingulate and salience network during rest in adolescents. J Child Psychol Psychiatry 52:1026–1034.

Treitz FH, Heyder K, Daum I (2007): Differential course of executive control changes during normal aging. Neuropsychol Dev Cogn B Aging Neuropsychol Cogn 14:370–393.

Turken AU, Swick D (1999): Response selection in the human anterior cingulate cortex. Nat Neurosci 2:920–924.

van Essen DC (2005): A Population-Average, Landmark- and Surface-based (PALS) atlas of human cerebral cortex. Neuroimage 28:635–662.

Walhovd KB, Fjell AM (2001): Two- and three-stimuli auditory oddball ERP tasks and neuropsychological measures in aging. Neuroreport 12:3149–3153.

Weissman-Fogel I, Moayedi M, Taylor KS, Pope G, Davis KD (2010): Cognitive and default-mode resting state networks: Do male and female brains "rest" differently? Hum Brain Mapp 31:1713–1726.

Xie C, Bai F, Yu H, Shi Y, Yuan Y, Chen G, Zhang Z, Li SJ (2012): Abnormal insula functional network is associated with episodic memory decline in amnestic mild cognitive impairment. Neuroimage 63:320–327.

Yan CG, Zang YF (2010): DPARSF: A MATLAB Toolbox for "Pipeline" data analysis of resting-state fMRI. Front Syst Neurosci 14:13.

Zhang H, Zuo XN, Ma SY, Zang YF, Milham MP, Zhu CZ (2010): Subject order-independent group ICA (SOI-GICA) for functional MRI data analysis. Neuroimage 51:1414–1424.

Zhou J, Greicius MD, Gennatas ED, Growdon ME, Jang JY, Rabinovici GD, Kramer JH, Weiner M, Miller BL, Seeley WW (2010): Divergent network connectivity changes in behavioural variant frontotemporal dementia and Alzheimer's disease. Brain 133:1352–1367.